

Magnetic pinning of flux lines in heterostructures of cuprates and manganites

J. Albrecht

*Max-Planck-Institut für Festkörperforschung, Heisenbergstrasse 1, D-70569 Stuttgart, Germany
and Max-Planck-Institut für Metallforschung, Heisenbergstrasse 3, D-70569 Stuttgart, Germany*

S. Soltan and H.-U. Habermeier

Max-Planck-Institut für Festkörperforschung, Heisenbergstrasse 1, D-70569 Stuttgart, Germany

(Received 25 April 2005; published 6 September 2005)

The magnetic properties of heterostructures of high-temperature superconducting $\text{YBa}_2\text{Cu}_3\text{O}_{7-\delta}$ and highly spin polarized, ferromagnetic $\text{La}_{2/3}\text{Ca}_{1/3}\text{MnO}_3$ that are electronically decoupled by a thin SrTiO_3 layer are investigated by means of SQUID magnetometry. Below the transition temperature of the superconducting component the detected signal is a measure for the critical current in the superconductor. The obtained magnetic hysteresis loops at low temperatures exhibit a substantial asymmetry with respect to $H=0$. This can be understood in terms of pinning of flux lines in the superconducting film due to magnetic interaction with the ferromagnetic manganite layer.

DOI: [10.1103/PhysRevB.72.092502](https://doi.org/10.1103/PhysRevB.72.092502)

PACS number(s): 74.78.Fk, 74.25.Qt, 74.72.Bk, 75.47.Lx

Heterostructures of superconductors and ferromagnets are of fundamental interest because at the interface between both materials a competition between different kinds of ordering phenomena occurs. In general, this leads to a reduction of the transition temperatures of both components. This effect increases strongly with decreasing thicknesses of the constituents.¹ However, if the thicknesses of the individual films increase and the interface-near volume fraction is small the transition temperatures are recovered. Nevertheless, there is still an interaction between superconductor and ferromagnet. One issue that will be addressed in more detail in this work is the influence of a neighboring magnetic layer on the pinning of the flux-line lattice of the superconductor.

The investigation of hybrid systems consisting of conventional superconductors and metallic ferromagnets has shown that it is possible to enhance the intrinsic flux line pinning in superconductors such as lead or aluminium enormously by the introduction of magnetic structures in vicinity of the superconductor.²⁻⁵ More recently, also high-temperature superconducting heterostructures are fabricated to explore similar phenomena in all-oxide systems. However, the characteristic length scales in high- T_c materials differ strongly from classical superconductors leading to weak magnetic pinning effects. The coherence length ξ of $\text{YBa}_2\text{Cu}_3\text{O}_{7-\delta}$ (YBCO) is about two orders of magnitude smaller than the magnetic penetration depth λ . All variations of the magnetic flux line energy are nearly smeared out over rather large length scales. Nevertheless, it has been found that specific high-temperature superconductor hybrid structures show effects of magnetic pinning. However, most effects are restricted to temperatures close to the transition temperature T_c where the intrinsic pinning of the superconductor is very weak.^{6,7} Only in epitaxial bilayers containing YBCO and ferromagnetic perovskites such as SrRuO_3 and LaCaMnO_3 substantial magnetic pinning was found at low temperatures so far.^{8,9}

In this Brief Report we present magnetization measurements of heterostructures consisting of thin films of YBCO and $\text{La}_{2/3}\text{Ca}_{1/3}\text{MnO}_3$ (LCMO) grown epitaxially on single-

crystalline substrates with lateral dimensions of $5 \times 5 \text{ mm}^2$ by pulsed laser deposition. Both films are electronically decoupled by a SrTiO_3 spacer layer with a thickness of 5 nm. The magnetization loops of these structures are obtained by SQUID measurements. These samples show a strongly asymmetric magnetic hysteresis loop in the whole temperature range below the superconducting transition. Similar curves are obtained for structures without decoupling layer.¹⁰ The measured diamagnetic signal has its origin in the magnetization of the superconductor created by supercurrents flowing in the YBCO layer. It is proportional to the pinning force density on the flux lines in this film. An asymmetric hysteresis loop indicates in this case a relationship between the magnetization state of the ferromagnet and the pinning in the superconductor in a wide temperature range.

All results are collected on samples that are produced using pulsed laser deposition. Single-crystalline [001] oriented substrates of SrTiO_3 (STO) and LaSrGaO_4 (LSGO) are used to grow thin LCMO films with a typical thickness of $d_{FM} = 50 \text{ nm}$. The important difference between the used substrate materials is the lattice constant which leads to a growth under *tensile* strain in case of the STO substrate and under *compressive* strain in case of the LSGO substrate.

To rule out any electronic interaction or spatially varying proximity effects that can lead to additional pinning effects¹¹ a thin layer of 5 nm STO is grown directly onto the LCMO film. The thickness of 5 nm is sufficient due to the small surface roughness of the LCMO film which was found in atomic force microscopy investigations to be below 1 nm. Finally, an optimally doped YBCO layer is grown on top with varying thicknesses d_{SC} between 50 and 150 nm. YBCO layers directly deposited on LCMO with thicknesses of 50 nm and more show a T_c of $T_c = 80 \text{ K}$ and above.¹² A sketch of the geometry of the used samples is given in Fig. 1.

In a first experiment the temperature-dependent magnetization of a sample consisting of an LCMO layer with a thickness of $d_{FM} = 50 \text{ nm}$, a 5 nm STO decoupling layer and a YBCO layer with a thickness of $d_{SC} = 100 \text{ nm}$ is shown in Fig. 2. The measurement has been performed after zero-field

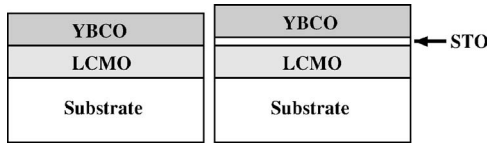


FIG. 1. Sketch of the geometry of the heterostructures. Left: An epitaxial bilayer of LCMO and YBCO. Right: Heterostructures of this work consisting of an LCMO layer, a decoupling STO layer with a thickness of 5 nm and a YBCO layer, all grown by pulsed laser deposition.

cooling to $T=5$ K in a magnetic field of $H_{ex}=10$ Oe. The orientation of the field is parallel to the film plane. The magnetization is measured with a SQUID magnetometer up to $T=300$ K (bottom curve) and back down (top curve) to $T=5$ K keeping the external field constant at $H_{ex}=10$ Oe.

The data in Fig. 2 show that the sample orders ferromagnetically at around $T=245$ K and at $T=87$ K a transition to superconductivity occurs. This can be seen from the diamagnetic signal occurring below $T=87$ K in the zero-field cooled measurement (bottom curve). This demonstrates that below $T=87$ K both superconducting and magnetic ordering appears in the sample.

We focus now on the critical current density of the superconducting film at low temperatures. For this purpose, a magnetic hysteresis loop measured at $T=5$ K is depicted in Fig. 3. The sample is cooled in zero field to $T=5$ K and an external field oriented perpendicular to the film plane is swept up to $H_{ex}=3$ kOe, then to $H_{ex}=-3$ kOe and back to $H_{ex}=3$ kOe again. The magnetization shows a behavior typical for a high-temperature superconductor with strong pinning. Starting at $H_{ex}=0$ a diamagnetic signal is found that is saturated around 100 Oe (virgin curve). At this field the superconductor achieves the fully flux penetrated state and the modulus of the magnetization $|M|$ is proportional to the critical current density j_c . If the critical current density was constant, a square-shaped hysteresis loop would be obtained. The decrease towards higher magnetic fields is related to field-dependent flux-line pinning. However, the loop in Fig. 3 is only symmetric with respect to the origin and asymmet-

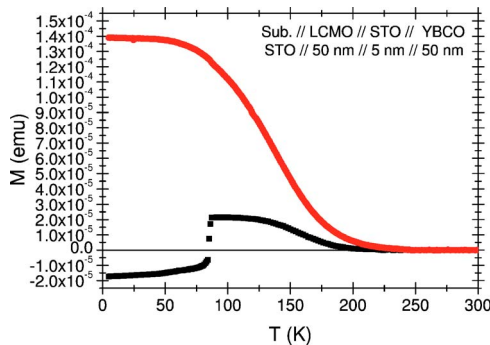


FIG. 2. (Color online) Temperature-dependent magnetization of a heterostructure of 50 nm LCMO and 100 nm YBCO, field-cooled (upper curve) and zero-field cooled (lower curve). The in-plane field for detection is $H_{ext}=10$ Oe. The results show ferromagnetic ordering at $T_{Curie}=245$ K and a superconducting transition at $T_c=87$ K.

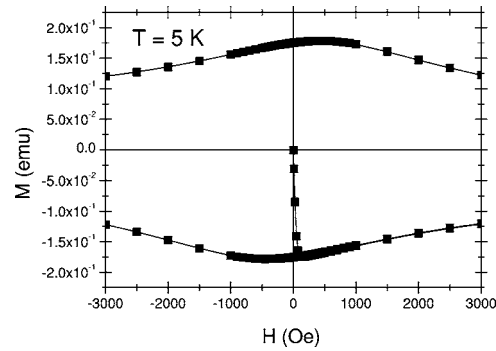


FIG. 3. Magnetization loop of a heterostructure consisting of 50 nm LCMO and 100 nm YBCO with decoupling layer obtained at $T=5$ K. The hysteresis loop shows no axial symmetry with respect to the vertical axis.

ric to the $M=0$ axis. The magnetization at a fixed external field clearly depends on the direction of the field sweep. This means not only the magnitude of the external field influences the current density also the direction of field changes plays a substantial role.

A possibility to extract this magnetic effect is summing up the two branches of the hysteresis loop and plotting the modulus of this sum. This process averages out the contribution of intrinsic pinning of the superconductor, only magnetic pinning remains. In case of homogeneous superconductors with high critical current densities and no weak links¹³ this magnetic pinning has to be introduced by the ferromagnetic film. The result is shown in Fig. 4. The value of $M^*=|M_1+M_2|$ is a measure of the difference of the critical current density which originates in different directions of field change or different magnetization states of the ferromagnet, respectively.

This curve shows two distinct maxima of M^* located symmetrically to $H=0$. The maximum value of M^* is $M^*=0.017$ emu which is about 10% of the magnetization. This difference can now be identified with the pinning of flux lines due to the vicinity of the ferromagnetic layer. Note, that this result still contains the reversible magnetization of the superconductor and the magnetization of ferromagnet and substrate, respectively. The reversible magnetization of the YBCO film has a maximum at H_{c1} which is for this thin film

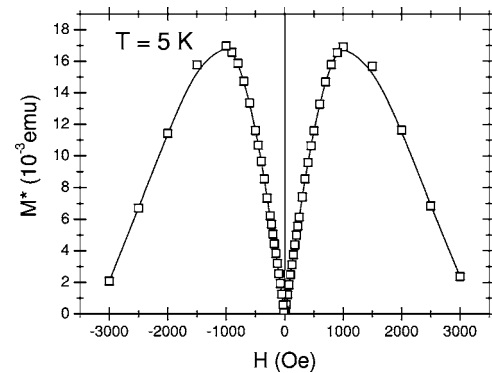


FIG. 4. Modulus $M^*=|M_1+M_2|$ of the sum of the two branches of the magnetization loop shown in Fig. 3.

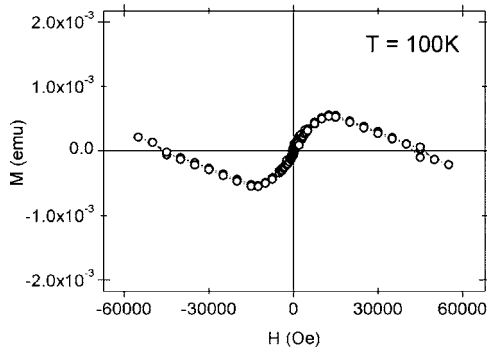


FIG. 5. Magnetization of the heterostructure at $T=100$ K.

geometry of the order of 10 Oe at $T=5$ K, this has not to be considered for the maxima at $H=1000$ Oe in Fig. 4.

To give an estimate for the contributions of ferromagnet and substrate Fig. 5 shows a magnetization loop up to $H=60\,000$ Oe above the superconducting transition temperature at $T=100$ K.

In Fig. 5 the contributions of ferromagnet and substrate can be identified. The magnetization of the LCMO saturates at $H \approx 15\,000$ Oe, at higher fields the linear diamagnetic signal of the substrate can be seen. At a field of $H=1000$ Oe (where the maxima show up in Fig. 4) the contribution of the LCMO layer can be extracted to be $M_{LCMO} \approx 1 \times 10^{-4}$ emu, the magnetization of the substrate is about $M_{Sub} \approx 2 \times 10^{-5}$ emu. The sum is less than 0.1% of the measured magnetization in Fig. 3 and less than 1% of the presented effect in Fig. 4.

It is not reasonable that the magnetizations of ferromagnet and substrate change by orders of magnitude between $T=100$ K and $T=5$ K, so we conclude that the observed effect is originated by magnetic pinning of the flux lines in the superconductor. The magnetic pinning force that acts on an individual flux line can be extracted by applying the Bean model on the magnetization data. This allows the determination of the critical current density in the superconducting film by assuming a homogeneous and constant current density throughout the whole sample. In case of the presented data of the bilayer consisting of a 100 nm YBCO film we find a critical current density of about $j_c \approx 1.0 \times 10^{11}$ A/m² which is in good accordance to magneto-optical measurements at systems without decoupling layer.⁹ Additionally, the corresponding magnetic pinning force on an individual flux line can be determined to $F_{pin} \approx 1.5$ pN. Similar values are found for magnetic pinning forces in interacting systems of ferromagnets and classical superconductors.¹⁴

The interaction of the flux line lattice in the YBCO film and the magnetic domain structure in the ferromagnetic LCMO depends, of course, strongly on the orientation of the domains. The local magnetization of a thin LCMO layer with a thickness of $d_{FM}=50$ nm can be influenced by using substrates with different lattice parameters to create various strain fields during epitaxial growth. It has been shown that LCMO thin films that grow under compressive strain show an out-of-plane orientation of the magnetization whereas a growth with no strain or under small tensile strain fields leads to an in-plane magnetization in these films.¹⁵ The ori-

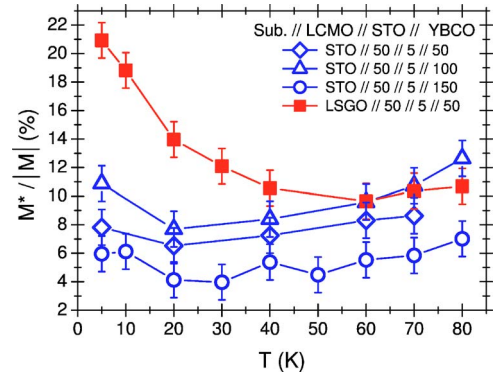


FIG. 6. (Color online) Temperature dependence of the magnetic pinning effect $M^*/|M|$ for different heterostructures. Samples grown on STO (open symbols) show a nearly constant effect over the whole temperature range, the heterostructure grown on LSGO (full squares) shows a different behavior.

entation of the easy axis of the LCMO film should therefore lead to different magnetic pinning properties of bilayers containing these manganite films. Figure 6 shows magnetic pinning $M^*/|M|$ for four different kinds of bilayers. First, the bilayer consisting of 50 nm LCMO and 100 nm YBCO grown on STO that already has been introduced in Figs. 3–5, second and third, the same structure with YBCO layers with $d_{SC}=50$ nm and $d_{SC}=150$ nm, respectively, and finally, a bilayer structure containing a 50 nm LCMO and a 50 nm YBCO film grown under compressive strain on a LaSrGaO₄ (LSGO) substrate.

The results in Fig. 6 clearly show that all structures grown on STO substrates under tensile strain show a similar behavior. For the two thinner structures we observe a nearly constant contribution of the magnetic pinning in the order of 10% over the whole temperature range. The thickest bilayer shows a temperature-independent magnetic pinning contribution of about 5% to 6% which can be understood concerning that the magnetic structures are smeared out over the thickness. A different behavior exhibits the structure grown under compressive strain on the LSGO substrate. At low temperatures we find a magnetic contribution to the flux line pinning of more than 20%, this value decreases monotonically to about $M^*/|M|=10\%$ above $T=50$ K. The increase of the effect in case of a perpendicular magnetization is predicted by theoretical considerations.¹⁶ The results presented in Fig. 6 directly show that a change of the domain pattern in the ferromagnet directly affects the properties of the magnetic pinning effect. This supports the model that the magnetic stray fields of the domain pattern in the ferromagnet cause a substantial pinning force density on the flux lines in the superconductor.

The presented results concern the flux pinning in bilayers while performing full hysteresis loops. It has been found in magneto-optical measurements that the critical current density in bilayers without decoupling layer exhibits strong differences between the zero-field cooled state and the field-cooled state.^{8,9} This effect should also appear in the virgin curve of the magnetic hysteresis loop. Although, one has to be careful because the magnetization is only a measure of the critical current density if the whole superconductor is in the

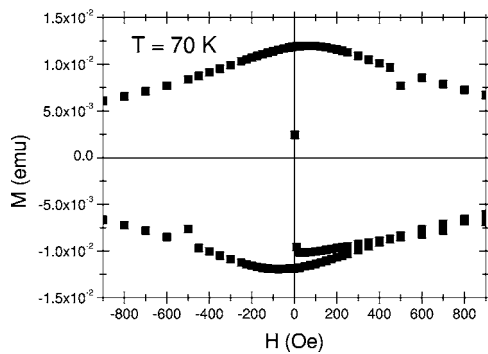


FIG. 7. Hysteresis loop of a 50 nm LCMO/5 nm STO/50 nm YBCO heterostructure on a STO substrate, obtained at $T = 70$ K. In this measurement a substantial reduction of the magnetization in the virgin branch occurs.

critical state, i.e., magnetic flux is fully penetrated into the sample.

Figure 7 shows the magnetization with respect to the external magnetic field for a bilayer with decoupling layer that consists of a 50 nm LCMO film and a 50 nm YBCO film grown on a STO substrate. The magnetization loop is measured at $T = 70$ K, at this temperature the fully penetrated state is achieved at an external field of about $H = 30$ Oe.

In contrast to the result presented in Fig. 3 a distinct difference between the virgin curve and the complete magnetization loop is found. The maximum of the magnetization in the virgin curve is about 25% smaller. This is related to the results that are found in the magneto-optical measurements of

bilayers without decoupling layer mentioned above. Up to now, this behavior cannot be explained in detail, it is suggested that the formation of the magnetic domains in the LCMO layer is strongly affected by the flux line lattice in the superconductor, especially at temperatures between $T = 50$ K and T_c of the YBCO film. Detailed knowledge about this mechanism can only be found by imaging the development of the domain structure under varying magnetic fields in these heterostructures which is not realized so far.

In summary, we have shown that the superconducting critical current density in bilayers consisting of high-temperature superconducting YBCO and ferromagnetic LCMO strongly depends on the magnetization state of the ferromagnetic layer. The contribution of magnetic pinning to the critical current density can achieve values of up to 30% and is present over the whole temperature range. Inserting a thin insulating layer in the bilayer structure leads to an electronic decoupling of both films and identifies the magnetic stray fields of the ferromagnetic layer as origin for the observed effects. It is found that a modification of the magnetic properties of the manganite layer by substrate induced strain fields leads to a change of the temperature dependence of the magnetic pinning force density.

ACKNOWLEDGMENTS

The authors are grateful to S. Brück for useful discussions and to G. Cristiani for the preparation of the excellent samples.

- ¹P. Prieto, P. Vivas, G. Campillo, E. Baca, L. F. Castro, M. Varelo, C. Ballesteros, J. E. Villegas, D. Arias, C. Leon, and J. Santamaria, *J. Appl. Phys.* **89**, 8026 (2001).
- ²Y. Jaccard, J. I. Martin, M. C. Cyrille, M. Velez, J. L. Vicent, and I. K. Schuller, *Phys. Rev. B* **58**, 8232 (1998).
- ³M. J. Van Bael, K. Temst, V. V. Moshchalkov, and Y. Bruynseraede, *Phys. Rev. B* **59**, 14674 (1999).
- ⁴S. Bending, G. D. Howells, A. N. Grigorenko, M. J. Van Bael, J. Bekaert, K. Ternst, L. von Look, V. V. Moshchalkov, Y. Bruynseraede, G. Borghs, and R. G. Humphreys, *Physica C* **332**, 20 (2000).
- ⁵M. Lange, M. J. Van Bael, V. V. Moshchalkov, and Y. Bruynseraede, *Appl. Phys. Lett.* **81**, 322 (2002).
- ⁶A. Garcia-Santiago, F. Sanchez, M. Varela, and J. Tejada, *Appl. Phys. Lett.* **77**, 2900 (2000).
- ⁷D. B. Jan, J. Y. Coultier, M. E. Hawley, L. N. Bulaevskii, M. P. Maley, Q. X. Jia, B. B. Maranville, F. Hellman, and X. Q. Pan, *Appl. Phys. Lett.* **82**, 778 (2003).

- ⁸J. Albrecht, S. Soltan, and H.-U. Habermeier, *Europhys. Lett.* **63**, 881 (2003).
- ⁹J. Albrecht, S. Soltan, and H.-U. Habermeier, *Physica C* **408-410**, 482 (2004).
- ¹⁰P. Przyslupski, I. Komissarov, W. Paszkowicz, P. Dluzewski, R. Minikayev, and M. Sawicki, *Phys. Rev. B* **69**, 134428 (2004).
- ¹¹M. Kienzle, J. Albrecht, R. Warthmann, H. Kronmüller, S. Leonhardt, and Ch. Jooss, *Phys. Rev. B* **66**, 054525 (2002).
- ¹²S. Soltan, J. Albrecht, and H.-U. Habermeier, *Phys. Rev. B* **70**, 144517 (2004).
- ¹³D. V. Shantsev, M. R. Koblischka, Y. M. Galperin, T. H. Johansen, L. Püst, and M. Jirsa, *Phys. Rev. Lett.* **82**, 2947 (1999).
- ¹⁴P. E. Goa, H. Hauglin, Å. A. Olsen, D. Shantsev, and T. H. Johansen, *Appl. Phys. Lett.* **82**, 79 (2003).
- ¹⁵T. K. Nath, R. A. Rao, D. Lavric, C. B. Eom, L. Wu, and F. Tsui, *Appl. Phys. Lett.* **74**, 1615 (1999).
- ¹⁶L. N. Bulaevskii, E. M. Chudnovsky, and M. P. Maley, *Appl. Phys. Lett.* **76**, 2594 (2000).